

UC Irvine

UC Irvine Previously Published Works

Title

Supernova relic neutrinos at Super-Kamiokande

Permalink

<https://escholarship.org/uc/item/9gd4395m>

Journal

Journal of Physics: Conference Series, 375

Authors

Bays, K.
Super-Kamiokande Collaboration, .

Publication Date

2012

DOI

10.1088/1742-6596/375/4/042037

Copyright Information

This work is made available under the terms of a Creative Commons Attribution License, available at <https://creativecommons.org/licenses/by/4.0/>

Peer reviewed

Supernova relic neutrinos at Super-Kamiokande

K. Bays and the Super-Kamiokande Collaboration

Department of Physics and Astronomy, University of California, Irvine, Irvine, California
92697-4575, USA

E-mail: kbays@uci.edu

Abstract. The diffuse supernova relic neutrino signal has never been observed. Currently the world's best upper flux limit comes from a search for inverse beta decay of anti-neutrinos in the Super-Kamiokande (SK) detector. A new SK study utilizes a novel method of spallation tagging, improved event selection, and an expanded data set to lower the analysis energy threshold and improve overall accuracy. Full results of this new study (including a combined upper flux limit of $2.8\text{--}3.1 \bar{\nu}_e \text{ events cm}^{-2} \text{ s}^{-1}$, $E_\nu > 17.3 \text{ MeV}$) are presented, as well as a short update on the research and development of using Gadolinium for neutron tagging.

1. Introduction

Neutrinos from core collapse supernovae throughout the history of the universe are expected to be reaching us today; all combined this is called the supernova relic neutrino (SRN) signal. Many astrophysicists have constructed models of this diffuse SRN signal; considered herein are some of these models (see Fig. 1) [1, 2, 3, 4, 5, 6].

The SRN signal has never been seen; the expected flux is only a few detectable events a year in SK. A paper was published in 2003 detailing the first search for the SRN events at SK and providing the world's most stringent flux limit [7]. We have now updated this result, with more livetime, a lower energy threshold, and significantly increased sensitivity.

Basic information about the SK detector can be found at [8]. SK can see $\bar{\nu}_e$'s via inverse beta decay. Three periods of SK data are considered herein: SK-I (1497 days livetime, 40% cathode coverage), SK-II (794 days, 19%), and SK-III (562 days, 40%).

2. Improvements to data reduction

To search for the SRN signal, a series of cuts is required to eliminate the numerous backgrounds. Even after all cuts, some backgrounds remain that must be modeled. The reconstruction software utilized is the same as in the long established SK solar analyses [9]. Many cuts are improved over the 2003 paper.

One of the most significant improvements is to the spallation cut. Cosmic ray muons enter the detector at $\sim 2 \text{ Hz}$, and can spall on oxygen nuclei to create radioactive isotopes. The amount of spallation increases sharply as energies fall below 20 MeV reconstructed total electron equivalent energy, and the average lifetime of spallation products tends to also increase as energy decreases, making spallation events harder to remove by correlating to the responsible muon. For these reasons, spallation is the dominant removable background $< 20 \text{ MeV}$, and determines the lower energy threshold of the analysis, as the final sample needs to be free of spallation contamination.

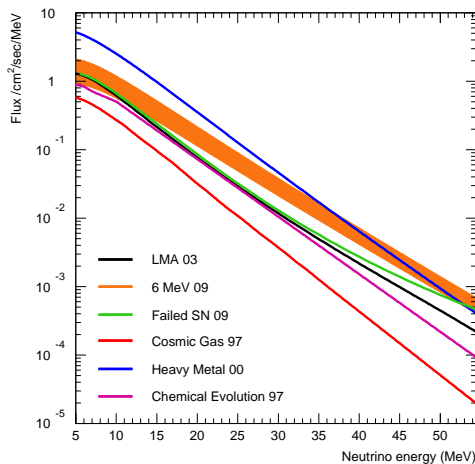


Figure 1. Examples of theoretical SRN spectra. Flux is $\bar{\nu}_e$ only.

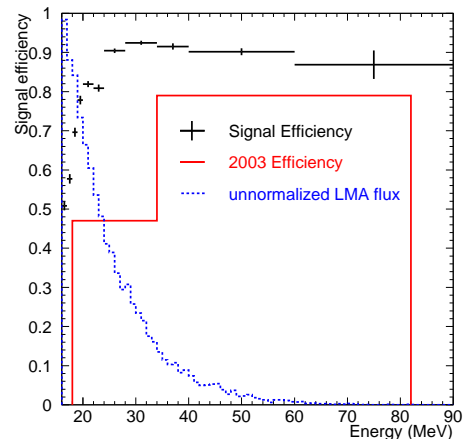


Figure 2. Signal efficiency of new analysis compared to 2003 study.

In the 2003 study, the lower energy threshold was set at 18 MeV total positron energy, and the cut was applied up to 34 MeV with an efficiency of 64%. This is now greatly improved by means of the following improvements: first, a new method of predicting where along the muon track the spallation is likely to occur has been developed, which corresponds to a peak in the dE/dx distribution of the muon track. This allows definition of a longitudinal distance, which is added as a likelihood in a new four variable spallation likelihood. Secondly, the muon track is now reconstructed using more precise reconstruction software that also categorizes the muon as a stopping muon, normal muon, or multiple muon bundle. Third, the four variable spallation likelihood is now tuned independently for each muon type. Altogether, these improvements allow reduction of the energy threshold from 18 MeV down to 16 MeV (17.5 MeV for SK-II), and improves the efficiency dramatically (from 64% to 91% for the data used in the 2003 study).

Also improved are the solar ν cut, pre and post-activity cuts, a new pion cut, and an incoming event cut, improving the total signal efficiency from 52% (18–82 MeV, SK-I data) to 79% (SK-I, 16–90 MeV), 69% (SK-II, 17.5–90 MeV) and 77% (SK-III, 16–90 MeV) (see Fig. 2).

3. Remaining backgrounds

After all cuts, a final sample remains, which is comprised of atmospheric ν backgrounds (and any SRN events). We model four backgrounds that play the most important role (other backgrounds exist but can be neglected). Only the first two of the backgrounds were considered in the 2003 study. The four backgrounds (see Fig. 3) are:

1: Atmospheric ν_μ CC events: This is the largest remaining background in our sample. Atmospheric ν_μ 's and $\bar{\nu}_\mu$'s create a muon via a charged current reaction. If the muon is below Cherenkov threshold its decay electron cannot be removed by correlation to the preceding muon. This background is modeled using decay electron data; all others use MC.

2: ν_e CC events: Atmospheric $\bar{\nu}_e$'s are indistinguishable from SN relic $\bar{\nu}_e$'s on an individual basis, and ν_e 's almost so. Their spectra are quite different, however.

3: Atmospheric ν neutral current (NC) elastic events: NC elastic scattering (on a nucleon) events have an energy spectrum that rises sharply at our lower energy bound, similar to SN relics. Most are removed by Cherenkov angle (C. angle) reconstruction, but some still leak into our final sample and must be modeled. With the lowering of the energy threshold from 18 MeV to 16 MeV, this background has become much more relevant.

4: μ/π production from atmospheric ν : This last category is a grouping of two heavier particles. First, NC reactions produce charged pions > 200 MeV/C, some of which survive the pion cut. Included with them, since the spectrum and C. angle distribution are relatively similar, are surviving muons above Cherenkov threshold.

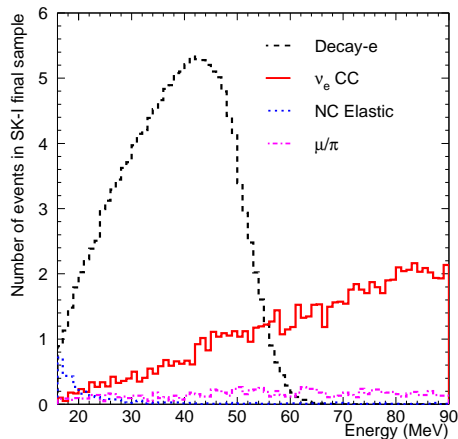


Figure 3. Remaining backgrounds in the signal region.

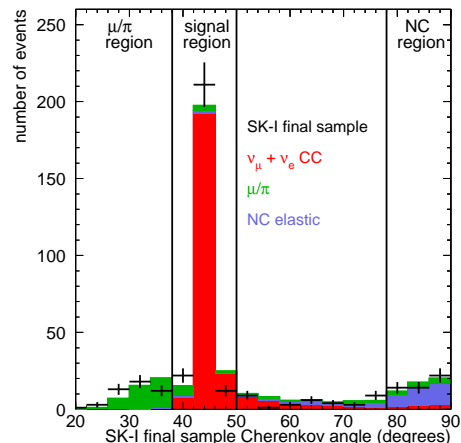


Figure 4. SK-I final sample and remaining backgrounds.

Figure 4 shows the C. angle of the four backgrounds, with no C. angle cut applied (from MC). While the CC backgrounds have a C. angle distribution similar to that of SN relics (which are almost all expected 38–50 degrees), the NC elastic background mostly reconstructs at high angles, and the μ/π events mostly reconstruct at lower angles (as expected from heavier, low energy particles). Because of these distributions, we have split the data into three regions: the signal region (38–50 degrees); and the two background regions, or ‘sidebands’, consisting of the low (20–38 degrees) μ/π region, and high (78–90 degrees) NC elastic region. The sidebands are used to normalize the NC elastic and μ/π backgrounds in the signal region.

4. Results

The relic best fit and upper flux limit are determined by performing an unbinned maximum likelihood fit simultaneously in all three C. angle regions. For each of the C. angle regions the spectrum of each of the five parameters (SN relic + 4 backgrounds) is parameterized into an analytical function, which is used as the PDF for that parameter. Each possible reasonable combination of parameters is checked; the likelihood in each C. angle region is separately calculated, but maximized in conjunction (for each SK data phase separately). If no statistically significant signal is seen, a 90% CL flux limit is extracted from the likelihood curve.

The following systematic errors are considered: cut inefficiency systematics, energy scale and energy resolution systematics, ν_e CC spectral shape error, and NC elastic normalization error.

No significant signal was seen in the data. SK-II and SK-III have a positive best fit, SK-I negative. Data with an example fit is shown in Fig. 3. Full results can be found in Table 1.

Also, SRN MC of various ν temperatures were created according to the prescription in [6, 11], allowing us to create an exclusion contour (Fig. 3) in two free parameters (by which most models can be well described): the ν luminosity of an average supernova, and the spectral shape assuming a Fermi-Dirac distribution and a particular ν temperature.

Table 1. 90 % CL flux limit ($\bar{\nu}$ cm⁻² s⁻¹), $E_\nu > 17.3$ MeV

Model	SK-I	SK-II	SK-III	All	Predicted
Gas Infall (97)	<2.1	<7.5	<7.8	<2.8	0.3
Chemical (97)	<2.2	<7.2	<7.8	<2.8	0.6
Heavy Metal (00)	<2.2	<7.4	<7.8	<2.8	< 1.8
LMA (03)	<2.5	<7.7	<8.0	<2.9	1.7
Failed SN (09)	<2.4	<8.0	<8.4	<3.0	0.7
6 MeV (09)	<2.7	<7.4	<8.7	<3.1	1.5

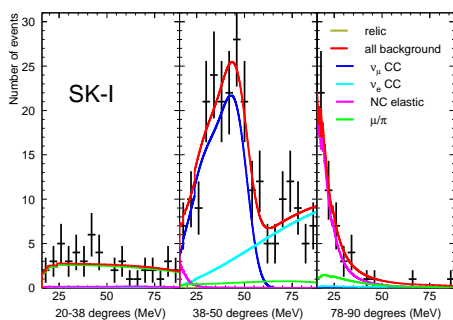


Figure 5. SK-I best fit result (LMA model shown).

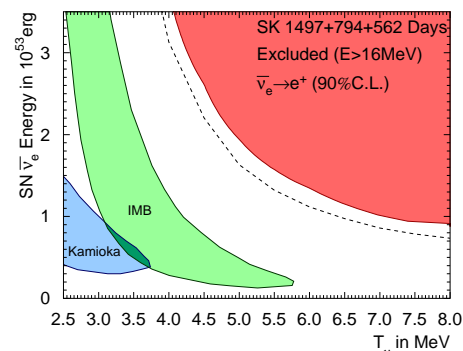


Figure 6. 90% CL exclusion; SN 1987A allowed regions from [10].

5. Gadolinium research

Future sensitivity improvements will be slow, since SK-I/II/III's exposure is already 176 kt-years, and the analysis is now highly optimized. The new SK-IV electronics structure may allow for some further background reduction, but clear discovery will likely require new methods, such as the doping of SK water with gadolinium, which could lower the energy threshold and backgrounds dramatically [12]. The feasibility of Gd doping in SK is currently under investigation in a new experiment located in a recently excavated cavity near the SK detector. This facility will be a small-scale replica of SK, using identical materials. A 200 ton test tank is already completed, along with a water system that effectively keeps the water ultra-pure without removing the Gd. PMTs will be installed early next year, and the intent is for this fully funded project to determine the feasibility of Gd doping in SK by the end of 2012.

- [1] Malaney R A 1997 *Astropart. Phys.* **7** 125–136
- [2] Hartmann D H and Woosley S E 1997 *Astropart. Phys.* **7** 137–146
- [3] Kaplinghat M, Steigman G and Walker T P 2000 *Phys. Rev. D* **62** 043001
- [4] Ando S, Sato K and Totani T 2003 *Astropart. Phys.* **18** 307–318
- [5] Lunardini C 2009 *Phys. Rev. Lett.* **102** 231101
- [6] Horiuchi S, Beacom J F and Dwek E 2009 *Phys. Rev. D* **79**(8) 083013
- [7] M Malek et al [Super-Kamiokande Collaboration] 2003 *Phys. Rev. Lett.* **90** 061101
- [8] Fukuda et al [Super-Kamiokande Collaboration] 2003 *Nucl. Instrum. Meth.* **A501** 418–462
- [9] J Hosaka et al [Super-Kamiokande Collaboration] 2006 *Phys. Rev. D* **73**, 112001
- [10] Jegerlehner B, Neubig F and Raffelt G 1996 *Phys. Rev.* **D54** 1194–1203 (*Preprint astro-ph/9601111*)
- [11] Beacom J F 2010 *Ann. Rev. Nucl. Part. Sci.* **60** 439–462 (*Preprint 1004.3311*)
- [12] Beacom J F and Vagins M R 2004 *Phys. Rev. Lett.* **93** 171101